

Design of X-joints in Sandwich Structures for Naval Vessels

Brian Hayman¹⁾, Christian Berggreen²⁾, Christian Lundsgaard-Larsen²⁾, Kasper Karlsen²⁾,
Claus Jenstrup²⁾

¹⁾ Section for Structural Integrity and Laboratories, Det Norske Veritas
Høvik, Norway
and Department of Mathematics, University of Oslo
Oslo, Norway

²⁾ Department of Mechanical Engineering, Technical University of Denmark
Kongens Lyngby, Denmark

Abstract

In many naval ships of fiber composite sandwich construction, an X-joint exists where the end bulkhead of the superstructure is attached to the deck, with an internal bulkhead placed in the same vertical plane below the deck. This joint is subjected to alternating tensile and compressive loading in the vertical direction for respectively hogging and sagging bending deformation of the hull girder. When the core material is polymer foam, such joints are often strengthened by the insertion of a higher density core material in the deck panel in the immediate region of the joint. The paper aims to improve the basis for the design of such X-joints, focusing on the prevention of crushing of the core under compressive load while ensuring adequate damage tolerance for the case of tensile load. Extensive material tests are reported, strain distributions are investigated by both laboratory tests and numerical modeling, and design guidance for core inserts is presented.

Keywords

Sandwich; X-joint; Debond; Fiber bridging; Core inserts.

Introduction

Sandwich construction with polymer foam core and face laminates of fiber reinforced plastics has been used in the hulls and superstructures of a number of naval ships where low weight has been an important factor. In several cases the superstructure does not cover the full length of the hull, and in some cases it also does not cover the full width. In such an arrangement, the end bulkhead of the superstructure is usually attached to the deck in a position lined up with a transverse bulkhead placed underneath the deck. This situation results in an X-joint configuration with the deck running continuously through the joint and the bulkheads connected to its face laminates (Fig. 1).



Fig. 1: Naval vessel in sandwich construction, illustrating typical location of X-joint

As the hull girder flexes due to motion of the ship in waves, compressive and tensile vertical loadings are exerted alternately on such an X-joint for respectively sagging and hogging bending deformation. The compressive loading may lead to crushing of the sandwich core within the deck as it passes through the joint, while the tensile loading tends to pull the upper face laminate off the deck. If this happens, the in-plane compressive strength of the deck panel may be significantly reduced, because the detached face laminate has little buckling capacity. Thus it is important to prevent these modes of failure through good detailing of the joint. An important aspect is to ensure that the core inside the deck panel has sufficient strength, and for this purpose it is common to use a higher density piece of core in the region of the joint than is used in the remainder of the deck panel. Damage at such joints has been observed in service, suggesting that current practice for joint design is inadequate.

A literature search has revealed an appreciable amount of research into the behavior and optimization of sandwich T-joints (e.g. Kildegaard, 1992; Efstatios and Moan, 1996; Toftegaard and Lystrup, 2005), but very little information about X-joints. On this basis it is tempting to conclude that X-joint design has up to now

been largely based on experience of testing and analysis of T-joints. As the X-joint is a “harder” detail than the T-joint, in the sense that the stresses are likely to be more concentrated and that possibilities for redistribution may be more limited, it is suggested that such a procedure may be unconservative and thereby an important cause of the observed joint failures.

Typical polymer foam core materials, such as the Divinycell “H” series of cross-linked PVC foams, have lower strength in compression than in tension. This is because, under compressive loading, the cells of such foams undergo crushing deformation with local buckling of the cell walls, while the tensile strength is governed more by the tensile strength of the cell walls. Thus, if the tensile and compressive loads are roughly equal, initial selection of material and extent for the core insert should be based on the compressive loading case. For tensile loading, however, it is important to ensure that a local stress concentration or an initial production defect or local damage will not reduce the strength unacceptably. The most relevant type of defect or damage to consider is a lack of bond between the sandwich face and core, commonly referred to as a debond.

The objective of the work reported in the present paper is to provide an improved basis for the design of such X-joints. The following aspects are addressed:

- Determination of stress distributions in X-joints under compressive loading, using both laboratory tests and numerical modeling, validation of the FE (finite element) modeling approach, and establishment of design criteria for core inserts (regarding both dimensions and material properties) to avoid core crushing.
- Determination of pull-off resistance for a range of face laminate / core combinations with debond defects, also using both laboratory tests and numerical modeling, to determine optimal material combinations and selection criteria to ensure that tensile loading will not lead to uncontrolled growth of the debond.
- Determination of relevant fracture mechanics parameters by advanced laboratory testing to support the pull-off resistance studies, taking account of the mode-mixity that arises in this scenario.

The studies on pull-off behavior are an extension of the previous work by Berggreen (2004) and Berggreen et al. (2007a), and include an investigation of the effect of including chopped strand and woven mats in the face-core interface when the laminates are made with non-crimp fabrics.

X-joint Configurations and Material Lay-ups

Two alternative designs of X-joint with GFRP face laminates and overlaminates and PVC foam core have been studied, with different fillet radii and overlamination details at the joint, see Fig. 2. The fillet radius (and thus the radius of the overlamination at the

joint) is an important design parameter (Kildegard, 1992), and influences the shape and extent of the compressive and tensile stress distributions in the core. Fig. 3 shows the geometry of the specimens used for testing of the X-joints under compression loading. Note that the overlaminations are shown in a schematic representation in Fig. 2 and Fig. 3. Wooden inserts have been used to reinforce the core at all loaded and free ends of the specimens. Five specimens of each type have been manufactured and tested.

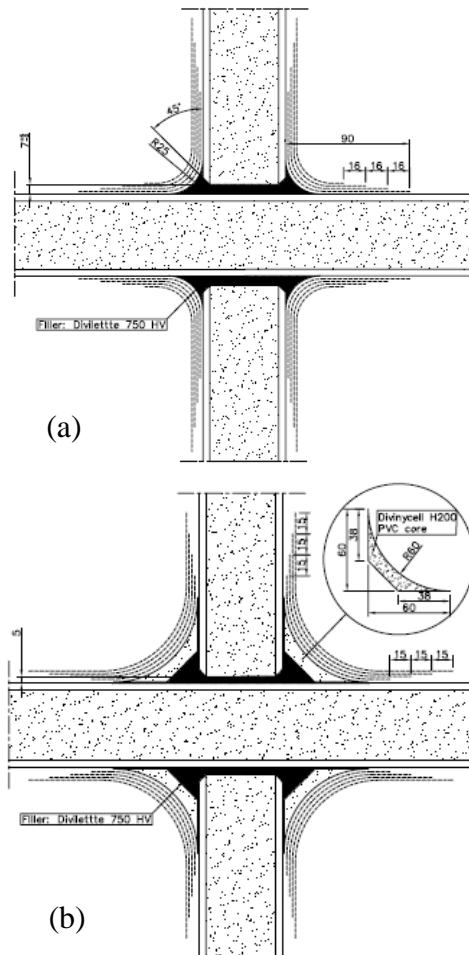


Fig. 2: Schematic representation of fillet and overlamination details. (a) Type X1. (b) Type X2

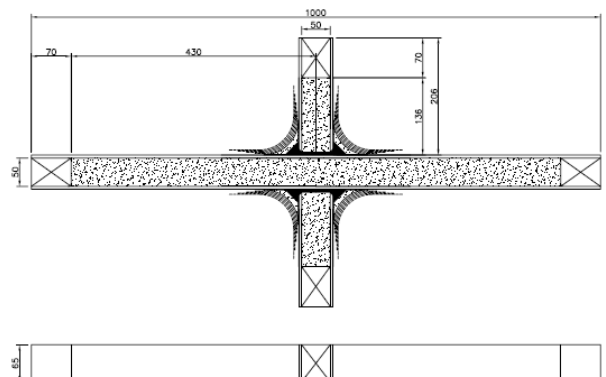


Fig. 3: Test specimen geometry. Shown for type X2, but type X1 has similar dimensions

In both X-joint specimen types, the face laminates each consist of four quadri-axial, E-glass mats (Devold AMT DBLT-850, 850 g/m²) in a (0/45/90/-45)_{2s} configuration, together with polyester resin (Polylite 720-691), manufactured using vacuum assisted resin injection. The resulting face thickness is approximately 3 mm.

The core is a 50 mm thick cross-linked PVC foam of the relatively heavy Divinycell H200 type, with a density of approximately 200 kg/m³. The filler Norpol FI 177-10 has been applied in all joints.

For the X1-type specimens the fillet radius is 25 mm and the overlaminations are made using E-glass fibre mats corresponding to the lay-up in the face laminates. The overlamination mats have a length of 150 mm and are placed staggered 16 mm in each layer relative to one another, as indicated in Fig. 2.

Apart from filler and overlaminations, the X2-type specimens also have a specially designed Divinycell H250 foam insert embedded in the filler material, thus increasing the fillet radius to 60 mm and reducing the weight. The fibre mats (same as for the X1 type) used for the overlaminations are of different length, increasing with 30 mm between each layer, i.e. four layers in all, in order to resemble the face laminate lay-up of the faces. The mats are placed symmetrically around the angle bisector of the fillet radius.

Determination of Material Properties

Face Laminate Properties

In the modeling studies, the face laminates and overlaminations were represented by a linear-elastic, orthotropic material model. In-plane material parameters (E-moduli and Poisson's ratio) were measured in tensile tests. The remaining in-plane and out-of-plane properties were estimated based on resin properties and an assumption of quasi-isotropic material behavior for the quadri-axial laminates. The applied material properties can be seen in Table 1.

Table 1: Mechanical properties for face laminates and overlaminations.

E ₁	E ₂	E ₃	v ₁₂	v ₁₃	v ₂₃
14.50 GPa	14.50 GPa	3.65 GPa	0.33	0.33	0.33
G ₁₂		G ₁₃		G ₂₃	
5.45 GPa		1.37 GPa		1.37 GPa	

Core Properties

To model the inelastic crushing and densification regimes of the H200 PVC foam core material, it was decided to use the crushable foam material model in ABAQUS. Extensive material tests were carried out to establish the material input parameters. The applicability of the foam material model was then checked by performing FE analyses of material specimens and comparing the results with those of the corresponding experimental tests. The resulting stress-strain relation assumed for the material model is shown

in Fig. 4. This displays an initial, linear-elastic regime with Young's modulus and Poisson's ratio 250 MPa and 0.32, respectively. A crushing regime follows, during which the stress increases more slowly with increasing strain. The strain at crushing initiation was found to be in the region of 2% for all the specimens tested. Finally, for strains above about 44% densification of the foam occurs.

These properties were obtained on the basis of samples taken from a single sheet of H200 core material. The density was found to vary significantly between these sheets and those used for the X-joint specimens. To allow for this the mechanical properties for the X-joint cores were scaled linearly with the density (DIAB, 2007). The elastic properties for the H250 foam fillets were based on datasheet values (DIAB, 2007) and the inelastic properties were scaled from the H200 material test results.

Details of the foam core material tests and modeling are given by Karlsen and Jenstrup (2007) and will be the subject of a later publication.

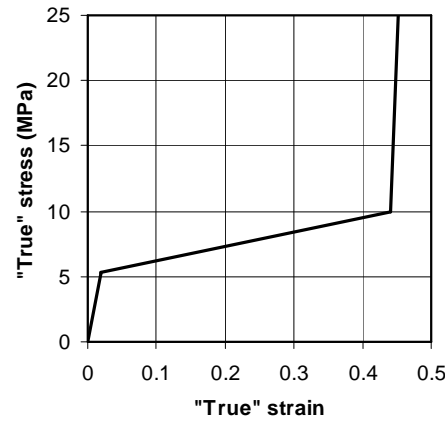


Fig. 4: Assumed stress-strain curve for H200 core material of density 240 kg/m³, based on test data.

Adhesive Filler Properties

The Reichhold NORPOL FI-177 adhesive filler was modeled as an isotropic, linear-elastic material. It was found that the compressive stresses in the adhesive filler do not reach the plastic yield limit during the analysis. The values assumed for Young's modulus and Poisson's ratio were 289 MPa and 0.30 respectively, in accordance with the manufacturer's data sheet.

X-joints under Compressive Loading

Load-deflection Curves and Strain Distributions

The deformations of the two X-joint designs illustrated in Fig. 2 have been investigated both numerically using a commercial FE-code (ABAQUS) and experimentally using advanced digital deformation measurements (Berggreen et al., 2007b).

The analyses were performed using a two-dimensional plane strain model as shown for the X1-type joint in Fig. 5.

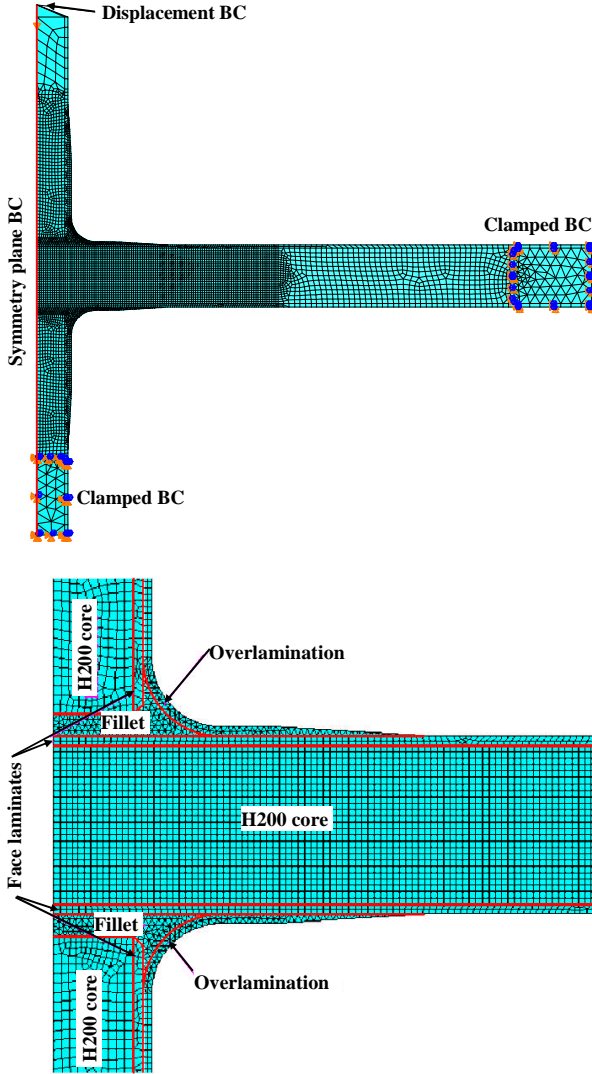


Fig. 5: FE mesh for X1 joint analysis, with enlarged view of central region.

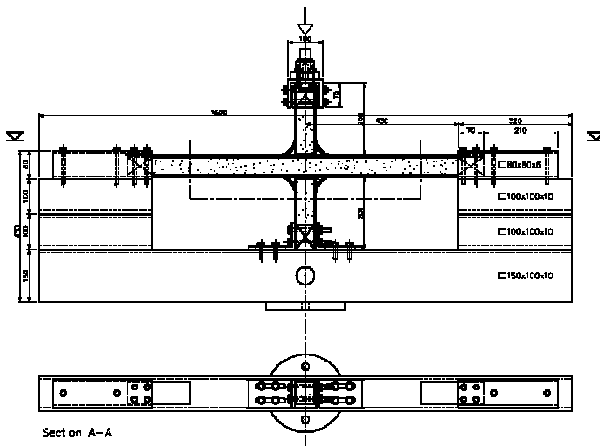


Fig. 6: Test specimen and arrangement for X-joint compressive loading tests.

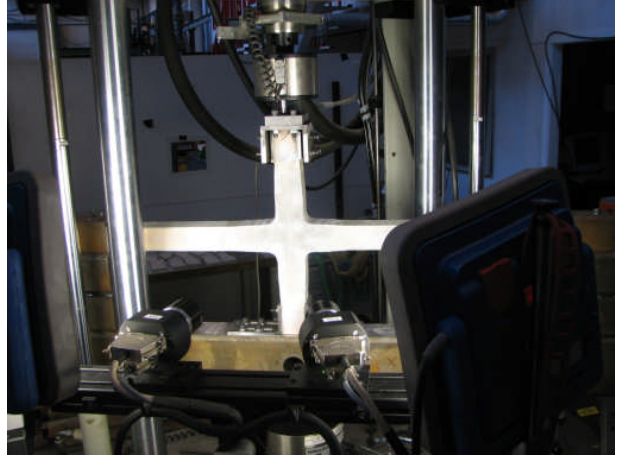


Fig. 7: Test rig with X1 specimen and digital cameras.

The test arrangement is shown in Fig. 6 and Fig. 7. The test rig was mounted in an Instron 8502 servo-hydraulic test machine. The ends of the horizontal and vertical sandwich elements were reinforced with hardwood inserts and rigidly clamped to the test rig fittings. Compression loads were introduced into the specimens at a displacement-controlled loading rate of 1.5 mm/min, and measured by a 100 kN load cell. (While the loading rates experienced by such an X-joint in practice may be somewhat higher than applied in these tests, strain rate effects are assumed not to have a major influence on the behavior.) Full-field displacements and surface strains were measured at one side of the specimen using an advanced digital optical system (ARAMIS 4M) operating at a frequency of 0.25 Hz.

Fig. 8 shows the load-displacement behavior for each of the joints as obtained from measurements and analyses. Good agreement was obtained between laboratory tests and FE calculations for strain distributions in the core of the horizontal deck panel and for the load-displacement response in the elastic range. Agreement was less good for the load-displacement response in the core crushing regime, though the initiation of core crushing was well predicted. As discussed by Berggreen et al (2007b), this may well be due to the necessity to assume plane strain deformation in the core crushing model, while the tested X-joints were in a condition closer to plane stress and developed significant out-of-plane distortion of the cross-sections (Fig. 9).

From the test results it is seen that the X1 joints first experience significantly non-linear behavior at a load of about 650 kN/m, when significant core crushing is developing. The load increases to about 750 kN/m before final failure occurs by separation of the overlaminates (Fig. 9). In the X2 joints the development of core crushing is more gradual, with non-linearity becoming evident at a load of about 800 kN/m and failure of the overlaminations at loads in the region of 1000 kN/m.

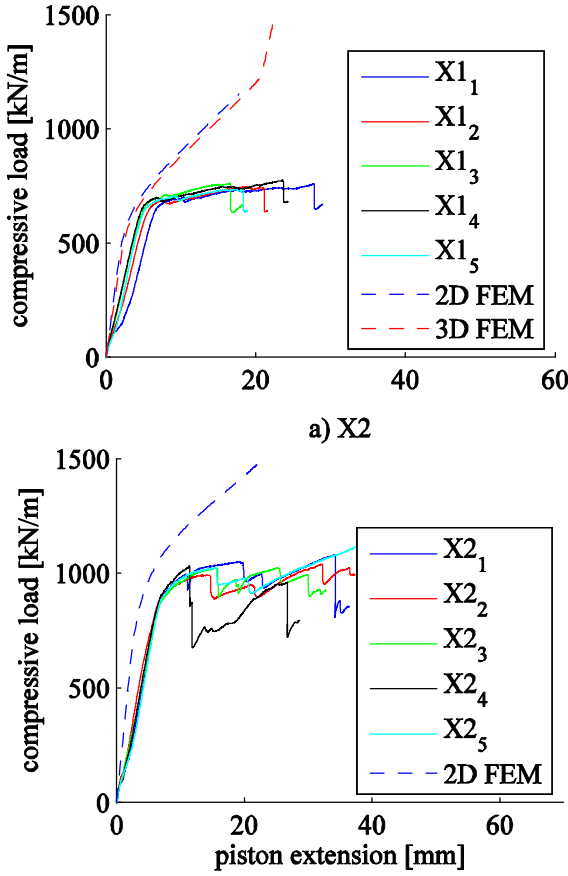


Fig. 8: Compressive load per unit width as a function of the applied vertical displacement for specimen types X1 and X2.

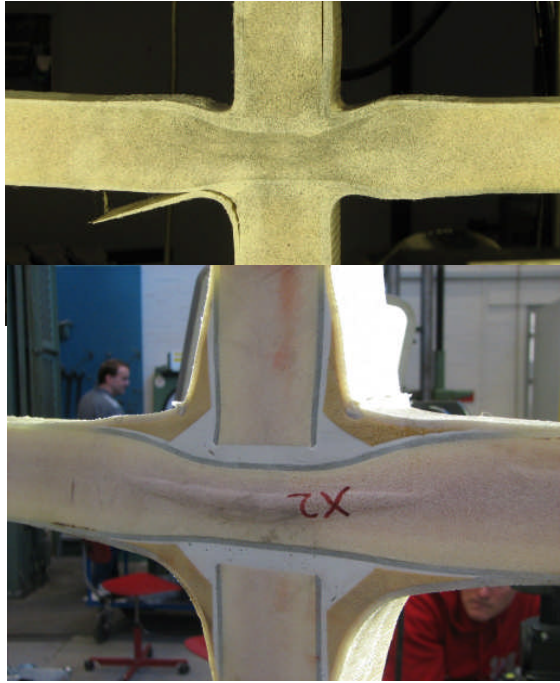


Fig. 9: Final failure of specimen X1₁ and large deformations in the core and failure of upper overlaminations in the X2₁ specimen

Conclusions for Selection of Core Material and Design of Core Inserts

Fig. 10 shows the von Mises strain as measured by the ARAMIS system on specimen X1₃ at a load of approximately 461 kN/m. Fig. 11 shows the maximum compressive principal strains, plotted against position along a series of horizontal section lines through the core of the deck panel, for each of the X1 joints at similar load levels within the elastic regime. The corresponding results from the FE analyses are also shown.

The section lines are defined in Fig. 10. With the exception of specimen X1₅, the test results show a reasonable degree of symmetry about the vertical symmetry axis of the specimens. A similar plot to those of Fig 11 is shown for section line 0 for the X2 joints in Fig. 12.

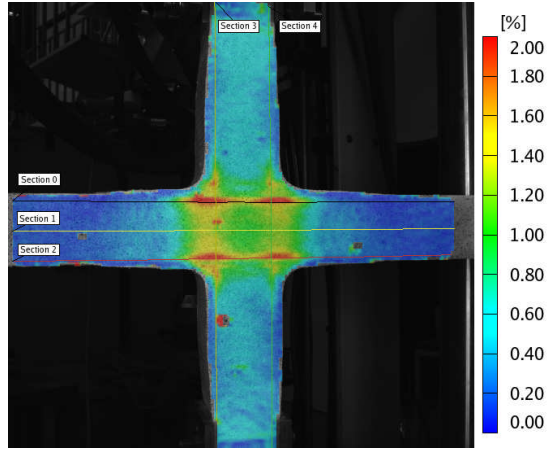


Fig. 10: Von Mises strains obtained by ARAMIS system for joint X1₃ at 461 kN/M, showing section lines used for data extraction.

Figs. 11 and 12 allow some conclusions to be drawn regarding the selection of core material for the joints. Firstly it is possible, by scaling these results or by studying the responses at successive load steps in the analysis, to deduce the loads at which crushing of the H200 core begins. This represents a limiting load beyond which some permanent damage may be expected in an X-joint having H200 foam core throughout the joint. Assuming that crushing of H200 foam core begins at a compressive strain of 2%, and basing the estimates on the FE analysis, gives the resulting limits for the X1 and X2 joints as approximately 550 kN/m and 715 kN/m respectively. For each type of joint the greatest compressive strain in the core occurs close to the upper face laminate of the deck panel just below the end of the face laminate of the vertical panel. The strain at the corresponding position above the lower face laminate is slightly smaller as a result of the asymmetry introduced by the clamping of the ends of the deck panel.

It is also possible to draw some tentative conclusions regarding designs with an insert of higher-strength core material in the most highly loaded part of the horizontal deck panel, as illustrated in Fig. 13. Two alternative cases may be considered: (a) when a higher strength

foam insert is to be used in a panel that is made otherwise with H200 foam core, and (b) when an H200 foam insert is used in a panel that is made otherwise with a lower strength foam.

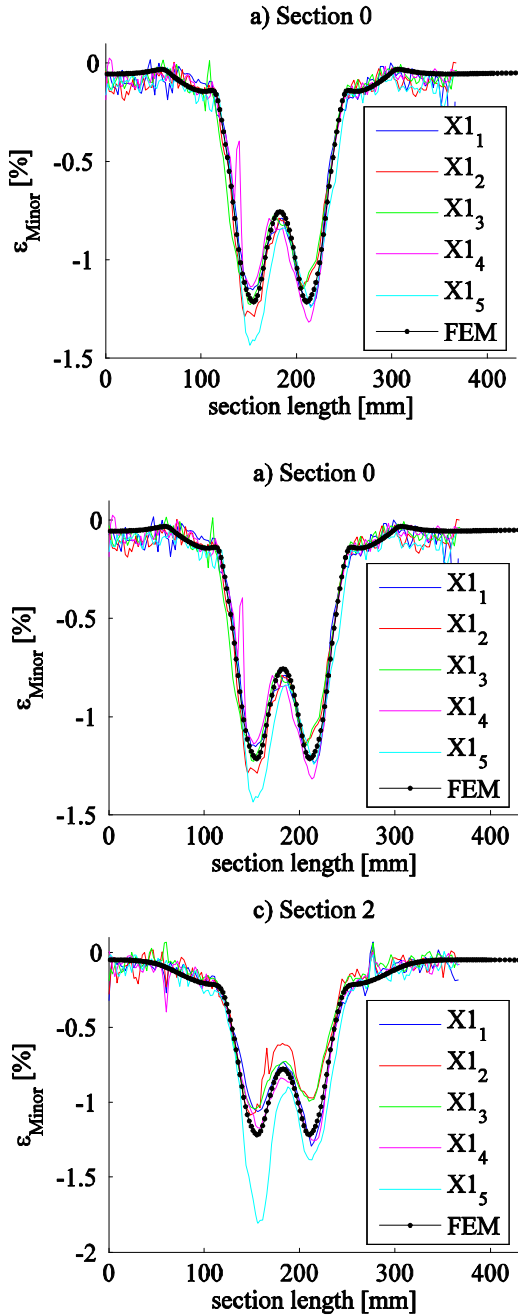


Fig. 11: Maximum compressive principal strains plotted along section lines for the X1 joints. Applied loads: $X1_1 = 310 \text{ kN/m}$, $X1_2 = 308 \text{ kN/m}$, $X1_3 = 318 \text{ kN/m}$, $X1_4 = 315 \text{ kN/m}$, $X1_5 = 315 \text{ kN/m}$, FEM = 333 kN/m.

(a) H200 Core with Higher Strength Insert

It is readily seen from Fig. 11 that the compressive strains, and hence the compressive stresses, in the core drop very rapidly at distances greater than about 50 mm to each side of the vertical centerline of the X1 joint, and become quite small at distances over about 70 mm. Thus, if a stronger material were substituted for the H200 foam over a total length of 100 mm or more, the

joint would be able to carry a greater load without suffering permanent damage to the core. With an insert length of 140 mm or more the increased capacity could be quite considerable. The strain level, and hence the stress level, in the core region outside the insert is then very much lower than in the central part of the insert, so the parameters determining the limiting load for the joint will be primarily the strength of the inserted core material and the strength of the other components in the joint, such as the overlaminations. Based on the observations in the tests, it is reasonable to suppose that the overlaminations etc. will be able to withstand a load of at least 700 kN/m, though this would need to be confirmed in the presence of an insert. An insert to support this loading without crushing would need to have the strength about 30% higher than H200.

The picture is similar for the X2 joint, though the rate, at which the compressive strains and stresses decline for increasing distance from the joint, is lower (Fig. 12). The length of insert needed to reinforce the entire region experiencing local stresses is now increased to about 190-200 mm, though some appreciable benefit would be gained with any insert length greater than about 100 mm.

For either type of joint, an accurate estimate of the limiting load can only be found by analyzing or testing the joint with the actual combination of core materials.

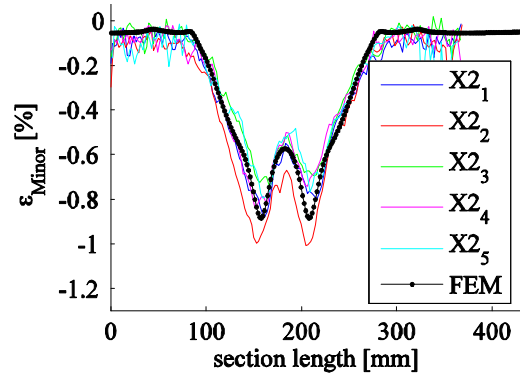


Fig. 12: Maximum compressive principal strains plotted along section line 0 for the X2 joints. Applied loads: $X2_1 = 317 \text{ kN/m}$, $X2_2 = 367 \text{ kN/m}$, $X2_3 = 311 \text{ kN/m}$, $X2_4 = 329 \text{ kN/m}$, $X2_5 = 314 \text{ kN/m}$, FEM = 320 kN/m

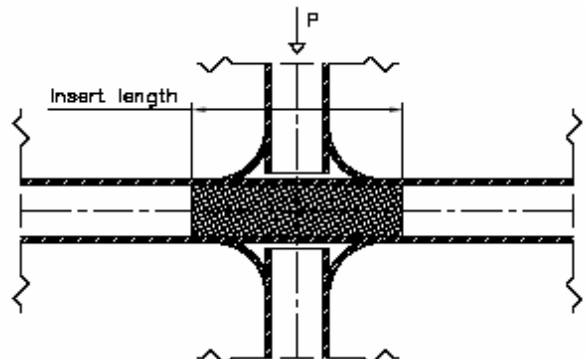


Fig. 13: Schematic layout of core insert in X-joint, with insert length definition.

(b) Lower Strength Core with H200 Insert

Similar conclusions may be drawn for the case when the core insert is of H200 material and the core outside the insert is a lower grade material. For the X1 joint a core insert of length 140 mm or more would ensure that the lower grade core material outside the joint was only lightly stressed, so it could be of appreciably lower strength without significantly influencing the limiting load for the joint. Furthermore, since the foam outside the insert is so lightly stressed, the substitution of a lower grade and lower-modulus material will not be expected to cause significant redistribution of stresses in the joint as compared to the case that has been analyzed and tested. The required strength of the lower grade core in the deck will now be determined by other loadings on the deck panel, while the joint capacity will be maintained at about 550 kN/m.

For the X2 joint, the same arguments may be used provided the insert length is 190 mm or more. Shorter inserts will give a benefit but this can only be quantified by testing or analysis of the configuration in question.

Further Consideration of the Insert Length

It is interesting to compare the required insert lengths described above with the geometry of the respective joints. For the X1 joint the thickness of the vertical panel extended by the radii of the two fillets and the widths of overlaminations before they start to taper down (about 17 mm each side) is 140 mm. For the X2 joint the corresponding dimension is approximately 192 mm. These dimensions agree extremely well with the length of the core region in the deck panel experiencing increased stresses, and thus the required insert length. However, this will not necessarily be the case for other joint designs.

Other Considerations

In addition to considering the modes of failure seen in the reported tests, it is necessary when selecting core inserts to consider the local stresses that are induced in the face laminates in the region of a joint between core blocks with differing stiffnesses, as shown by Bozhevolnaya et al. (2005) and Lyckegaard et al. (2006). Such stresses could be checked by means of FE analysis carried out on a joint with core insert.

X-joints under Tensile Loading

An X-joint located at the connection between a deck and a superstructure end bulkhead is subjected to similar tensile and compressive load levels if the hull girder hogging and sagging moments are roughly equal. As the tensile strength of the foam core material is higher than its compressive strength, the critical regions of the deck panel for tensile loading on the X-joint are then the core-laminate interfaces and the laminates themselves. (The strength of the connections between the vertical bulkheads and the deck face laminates will not be addressed here.) As the pull-off strength of the core-laminate interface and through-thickness tensile strength of the face laminate are sensitive to initial defects in the

form of debonds or delaminations it is of interest to study ways of ensuring an acceptable level of defect/damage tolerance in this region. The study by Lundsgaard-Larsen et al. (2007), which uses cohesive zone modeling in a FE analysis, combined with laboratory test results obtained by Karlsen and Jenstrup (2007), allows some conclusions to be drawn regarding the selection of materials and design of the joint.

Materials Considered in Damage Tolerance Studies

Four different laminate lay-ups were considered in the damage tolerance studies:

- I: 4 x DBLT850 as in the compression load studies
- II: As I but with a 450 g/m² layer of chopped strand mat (CSM) at the interface
- III: As II but with an additional layer of woven mat (tex68) between the DBLT850 and the CSM
- IV: As III but without the CSM

Fracture Toughness and Cohesive Laws

A detailed description of the FE modeling carried out by Lundsgaard-Larsen et al. (2007) using cohesive zone modeling at the sandwich core/face interface is beyond the scope of the present paper. Extensive fracture mechanics testing under mixed-mode conditions was performed by Karlsen and Jenstrup (2007) to obtain parameters for the cohesive model and to compare the performance of different face laminate lay-ups when combined with Divinycell H200 foam core. The test method was based on a Double Cantilever Beam specimen loaded by Uneven Bending Moments (DCB-UBM), see Sørensen et al. (2006). The FE modeling focused on lay-up II only. The other lay-ups showed behavior that indicated that the J-integral method used for developing the cohesive zone model would be invalid.

Pull-off Tests on Debonded Sandwich Beams

To simulate the tensile loading case on an X-joint without the complication of possible failure in the overlaminations, a series of pull-off tests was carried out on sandwich beams representing the horizontal deck panel with a debond between the upper laminate and the core (Lundsgaard-Larsen et al., 2007; Karlsen and Jenstrup, 2007). The sandwich specimen was mounted in the same test-rig as used for the compression testing, and loaded by an Instron 8502 servo-hydraulic test machine, see Fig.14. The replacement of the lower bulkhead portion by a rigid attachment is believed to have a minor effect on the behavior.

The middle of the bottom face is fixed to the test rig, and the middle of the top face is clamped to the cross-head as shown. The sandwich specimen has wooden inserts at the ends which are clamped to the test rig. A Teflon film is inserted between the upper face and core along half the specimen length, so that the crack will only propagate to one side and hence only one fracture incidence will occur in the measurements. The half of the beam with the Teflon film incorporated maintains some symmetry, and prevents excessive horizontal forces from being exerted on the piston of the test

machine. The displacement field of the specimen surface was recorded using the ARAMIS optical system as in the compression tests.

The specimen was loaded by moving the cross-head upwards with a rate of 2 mm/min. The face laminate had to be lifted 30-40 mm before the crack had fully propagated to the end support. During this time the crack propagated slowly, with an increasing amount of fiber bridging. A specimen with a fully propagated crack is seen in Fig. 15.

During each test the lift as measured by the test machine piston displacement, the lift force as measured by the load cell and the crack length found by tracking the opening between the core and face at different locations along the interface were all recorded. Five specimens of each of the types I – IV were tested. Each specimen had a width of 60-67 mm.

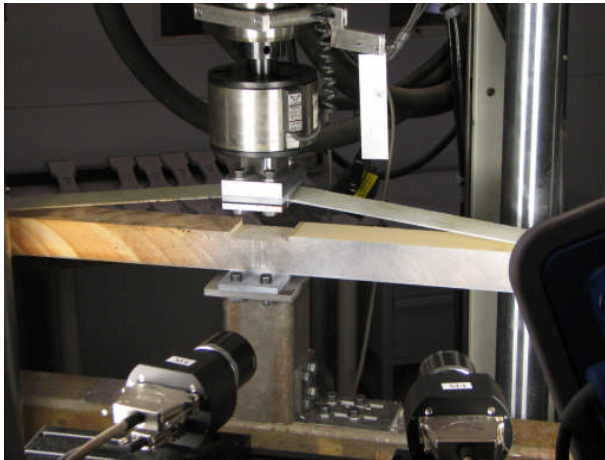


Fig. 14: Loaded beam specimen in tensile test machine.

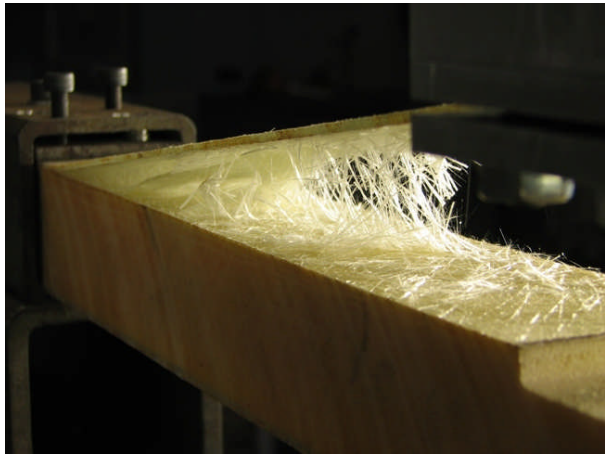


Fig. 15: Tested beam specimen with fibre bridging between the crack faces.

FE Modelling

A 2D finite element model was created using ABAQUS version 6.6 and the explicit solver was used. Due to symmetry only half the specimen was modeled. A schematic illustration of the model, with dimensions, is given in Fig. 16.

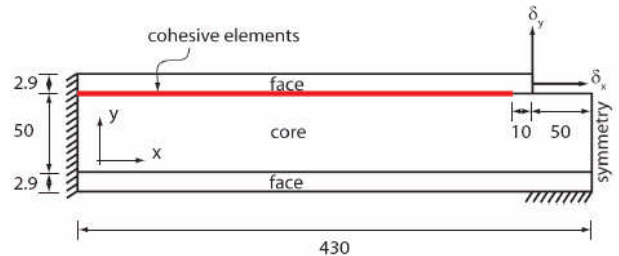


Fig. 16: Schematic drawing of the finite element model indicating boundary conditions, cohesive section and loading points.

The model consists of two faces and a core, where the top face and the core are connected through zero-thickness cohesive elements which represent the traction-separation behavior in the interface. The left edge of the sandwich beam is fixed, and the right edge is exposed to symmetry conditions. A length of 50 mm of the bottom right edge is fixed, since this part is clamped to the test rig in the experiments.

The finite element model is meshed uniformly with 4-noded bilinear rectangular elements each with 8 degrees of freedom. The element size is approximately 0.5 mm, which corresponds to 6 elements through the thickness direction of the face. The sandwich specimen is loaded in displacement control so that the edge of the face is displaced as shown in Fig. 16.

Analysis and Test Results for Pull-off Tests

For the purposes of assessing damage tolerance, and for considering the design of a core insert block, it is relevant to evaluate the results in terms of a plot of lift force against crack length. Fig. 17 shows such a plot as obtained by testing and FE analysis for the type II beams. The lift force reaches a local maximum just before the crack starts propagating, which is in good agreement with the results obtained in Berggreen et al. (2007a). It is seen that the FE analysis over-predicts this initial peak load, but that agreement improves as the crack propagates. Fig. 18 shows the averaged results for each specimen type. Here the forces have been divided by the specimen width.

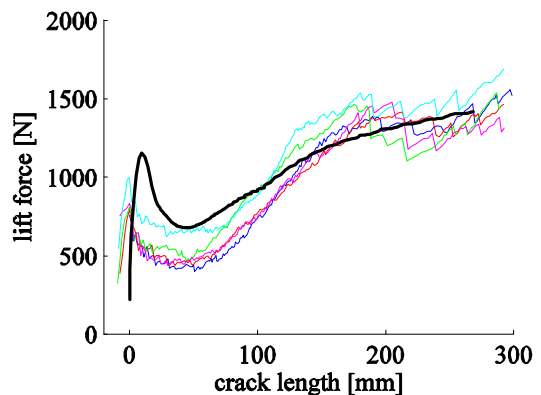


Fig. 17: Lift force as function of crack length for type II lay-up. The FE results are shown by the thick curve.

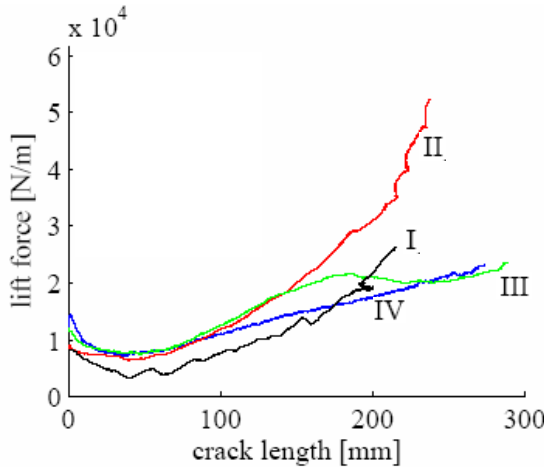


Fig. 18: Lift force per unit width as function of crack length: Average values for each specimen type

Conclusions from Pull-off Tests

Both the pull-off tests and the FE analyses show that, with H200 core, crack lengths of 100-200 mm are needed before the beneficial effects of fiber bridging raise the load capacity to the initial value it had before crack propagation began. The exact extent depends on the laminate lay-up.

The differences between the lay-ups can be at least partly explained as follows. The two interfaces without CSM, types I and IV are relatively brittle and show little or no fiber bridging. Lay-ups II and III, with CSM, give a tougher interface with fiber bridging. However, in case II the crack is seen to kink into the laminate so that further crack propagation results in even more effective fiber bridging but at the same time weakening the main load-carrying laminates. This contrasts with type III, for which the crack remains in the CSM. The type II lay-up also has the disadvantage that propagation begins at a relatively low load level.

The use of a CSM layer clearly has only a modest effect on the performance, as it only initiates scattered fiber bridging and the load carried by bridged fibers is limited by the length of each of the chopped fibers in the mat. It is possible that the use of continuous strand mat, with a layer of randomly arranged continuous fibers in place of the CSM, may increase the magnitude of the load that can be carried by the bridged fiber. This will be investigated in the next stage of the studies.

Implications for Core Insert Design

Attention is focused on the case when a block of H200 material is to be inserted in a core of lower grade material. The first item to note is that the load levels reached in the pull-off tests are of the order 10- 50 kN/m, which are very much lower than in the compression tests. The tension load that could be applied to a complete X-joint, however, would be greater because in the beam tests the face laminate on one half of the beam was already separated from the core. This part of the beam provides no resistance to lifting at small crack lengths, but as the lift increases there is an increasing contribution from the membrane

tension in the laminate itself. Thus the load applied to a complete X-joint would be approximately twice that measured in the beam tests initially, but the ratio reduces somewhat for larger crack lengths.

The second observation is that the required insert length to gain any benefit from the fiber bridging at large crack lengths are 200-400 mm depending on the lay-up. (Note that the required insert lengths are twice the single crack lengths at which the benefits are seen.) These lengths are similar to or greater than the lengths that typically emerged from the compression case.

The main conclusions from the damage tolerance studies are thus that the lay-ups with CSM at the interface provide the best damage tolerance in combination with an H200 core, and that fiber bridging will ensure that this damage tolerance is activated provided the H200 core extends over a width of at least 200 mm, which is similar to the minimum width required for the compression case. However, the tensile capacity of the joint with a debond defect is considerably lower than the compressive strength.

Conclusions

The laboratory tests and FE analyses have provided useful information for assessing the load-carrying performance of foam core materials and laminate-core interfaces in sandwich X-joints, and in particular for determining the required lengths of higher-strength blocks to be inserted in the through-going panel to avoid compressive core failure. The FE analyses reproduce the essential features of the behavior for both compression and tension loading cases, though quantitative agreement is best for the compression case.

The tensile load-carrying capacity of X-joints with face-core debond defects is limited but can be influenced by the choice of reinforcement adjacent to the interface. Further studies are planned in this area.

The studies reported here are limited to in-plane compressive and tensile loading on the bulkhead panels that are perpendicular to the through-going deck panel. These are considered to be the primary loads experienced by an X-joint connecting a superstructure end bulkhead, deck panel and internal bulkhead below the deck. The effects of shear and bending loadings may also need to be considered in some cases. A further phenomenon that is not considered here is the possibility of growth of a face-core debond under repeated loading; this type of damage growth is the subject of ongoing research.

Acknowledgements

This work has been performed within the context of the Network of Excellence on Marine Structures (MARSTRUCT), partially funded by the European Union through the Growth Programme under contract TNE3-CT-2003-506141. The provision of test specimens and materials by Kockums AB (Karlskronavarvet) and DIAB AB is highly appreciated.

References

- Berggreen, C (2004). "Damage Tolerance of Debonded Sandwich Structures", PhD Thesis, Technical University of Denmark, Department of Mechanical Engineering.
- Berggreen, C, Simonsen, BC and Borum, KK (2007a). "Experimental and numerical study of interface crack propagation in foam-cored sandwich beams. Journal of Composite Materials", Journal of Composite Materials, 41(4):493-520
- Berggreen, C, Lundsgaard-Larsen, C, Karlsen, K, Jenstrup, C and Hayman, B (2007b). "Improving performance of polymer fibre reinforced sandwich X-joints in naval vessels – Part I: Design aspects", 16th Int. Conf. on Composite Materials, Kyoto, Japan.
- Bozhevolnaya, E, Lyckegaard, A and Thomsen, OT (2005). "Localized Effects Across Core Junctions in Sandwich Beams Subjected to In-Plane and Out-of-Plane Loading", Applied Composite Materials, Vol.12, pp. 135-147.
- DIAB (2007). "Technical Manual – Divinycell H", <http://www.diabgroup.com/europe>.
- Efstathios, E and Moan, T (1996). "Experimental and numerical study of composite T-joints", Journal of Composite Materials, Vol. 30, No. 2, 190-209.
- Karlsen, K and Jensrup, C (2007). "Design of core inserts in sandwich X-joints – Experimental and numerical analysis", MSc Thesis, Department of Mechanical Engineering, Technical University of Denmark.
- Kildegaard, C (1992). "Experimental and numerical fracture mechanical studies of FRP-sandwich T-joints in maritime constructions", 2nd Int. Conference on Sandwich Constructions, Gainesville, USA.
- Lundsgaard-Larsen, C, Berggreen, C, Karlsen, K, Jenstrup, C and Hayman, B (2007). "Improving performance of polymer fibre reinforced sandwich X-joints in naval vessels – Part II: Damage Tolerance", 16th Int. Conf. on Composite Materials, Kyoto, Japan.
- Lyckegaard, A, Bozhevolnaya, E and Thomsen, OT (2006). "Parametric Study of Structurally Graded Core Junctions", Journal of Sandwich Structures and Materials, Vol. 8, No.5.
- Sørensen, BF, Jørgensen, K, Jacobsen, TK and Østergaard, RC (2006). "DCB-specimen loaded with uneven bending moments", International Journal of Fracture, Vol. 141, No. 1-2, pp 163-176.
- Toftegaard, H and Lystrup, A (2005). "Design and test of lightweight sandwich T-joint for naval ships". Composites: Part A, Vol. 36, No. 8, 1055-1065.